Original article

Folia Neuropathologica

Electrospun nanofiber mat as a protector against the consequences of brain injury

Dorota Sulejczak[1], Jarosław Andrychowski[2,3], Tomasz Kowalczyk[4], Paweł Nakielski[4], Małgorzata Frontczak-Baniewicz[5], Tomasz Kowalewski[4]

[1]Department of Experimental Pharmacology, Mossakowski Medical Research Centre, Polish Academy of Sciences, Warsaw, [2]Department of Neurosurgery, Medical University of Warsaw, Bielanski Hospital, Warsaw, [3]Department of Neurosurgery, Mossakowski Medical Research Centre, Polish Academy of Sciences, Warsaw, [4]Institute of Fundamental Technological Research, Polish Academy of Sciences, Warsaw, [5]Electron Microscopy Platform, Mossakowski Medical Research Centre, Polish Academy of Sciences, Warsaw, Poland

Folia Neuropathol 2014; 52 (1): 56-69 DOI: 10.5114/fn.2014.41744

Abstract

Traumatic/surgical brain injury can initiate a cascade of pathological changes that result, in the long run, in severe damage of brain parenchyma and encephalopathy. Excessive scarring can also interfere with brain function and the glial scar formed may hamper the restoration of damaged brain neural pathways. In this preliminary study we aimed to investigate the effect of dressing with an L-lactide-caprolactone copolymer nanofiber net on brain wound healing and the fate of the formed glial scar. Our rat model of surgical brain injury (SBI) of the fronto-temporal region of the sensorimotor cortex imitates well the respective human neurosurgery situation. Brains derived from SBI rats with net-undressed wound showed massive neurodegeneration, entry of systemic inflammatory cells into the brain parenchyma and the astrogliosis due to massive glial scar formation. Dressing of the wound with the nanofiber net delayed and reduced the destructive phenomena. We observed also a reduction in the scar thickness. The observed modification of local inflammation and cicatrization suggest that nanofiber nets could be useful in human neurosurgery.

Key words: *brain injury, L-lactide-caprolactone copolymer nanofiber net, glial scar, neurodegeneration.*

Introduction

Traumatic brain injury (TBI) and its sequels constitute a serious, critical public health and socioeconomic problem throughout the world. It is the most important cause of mortality and disability mostly among young population in the world because of different causes of trauma, i.e. the rising number of motor vehicle accidents [4,5,14,18,21]. This is the problem not only in the highly developed countries, but in other countries, too. There are short- and long-term aspects of clinically visible consequences of TBI. The instant or early posttraumatic consequences are monitored and treated after hospital admission; many of them are caused by neurosurgical interventions. Long-term consequences of TBI, or so-called posttraumatic syndrome, was divided to three major categories, physical, cognitive and psychological [17]. The progress of posttraumatic long-term consequences of the above mentioned diseases is unpredictable. It is known that even very minor brain damages can

Communicating author:
Dorota Sulejczak, Department of Experimental Pharmacology, Mossakowski Medical Research Centre, Polish Academy of Sciences, 5 Pawinskiego Str., 02-106 Warsaw, Poland, phone: +48 22 608 65 81, fax: +48 22 608 65 90, e-mail: dsulejczak@imdik.pan.pl

result in the most severe symptoms, conditions and consequences [13,23,31,33,34].

Another aspect to discuss is the potential trauma of post-surgical interventions due to the changes in the region of preparation, described as an oedematous or vascular lesion. Obviously, the neurosurgical interventions to the brain should be minimally invasive, which means avoiding additional brain trauma, using safety entrance region to the lesions, avoiding inappropriate microsurgical manoeuvres. However, the posttraumatic brain injury and micro trauma after surgery can induce and initiate pathological machinery into parenchyma and possible potential cascade of changes that result, in the long run, in progressive tissue damage [24]. After trauma, unfortunately there is no efficient neuroprotective treatment avoiding inflammatory response and this information is crucial for developing preventive and new treatment strategies.

It is known that the scar tissue can be formed as a consequence of injuries or damages such as tumour or traumatic brain injury. Brain scar tissue can obstruct proper healing and brain function and may slow the nerve regeneration in the brain. It is known that disrupted nerve growth results in neural dysfunctions. This is the cause of symptoms in patients with brain damage involving the scar. Additionally, untreated scar can further worsen the brain function.

One of the possibilities to remove brain scar tissue is to eliminate it by surgery. However, depending on where the scar tissue is located and how much it is, not all of it may be removed. New technologies, such as nanotechnology, provide a variety of different treatment options of getting rid of the brain scar tissue as well as encouraging brain nerve regrowth.

In our earlier studies we used a rat model of surgical brain injury (SBI) for investigating the consequences of brain damage and scar formation [9]. In this animal model, the SBI is done by excising a moderate-sized piece of sensorimotor cerebral cortex. This model imitates well the respective human neurosurgery situation in that it involves the most typical early consequences of TBI, such as brain oedema and neuronal death. The changes are very similar to those observed following brain ischemia [15,35].

The electrospinning has been known since the 1930s. It is a comparably cheap and versatile method of production of micro- and nanofibers of a diameter ranging from a few micrometers to a few nanometres. In the process, a fluid filament is stretched in a strong electric field and produces material that is collected as a nonwoven mat of micro- and nanofibers. Biomedical applications of nanofibers are concentrating on a unique property of micro- and nanofibers – they can mimic extracellular collagen matrix (fibrils size of 50-500 µm) [1]. The membranes are colonized by cells and nativized. If nanofibers are produced from biodegradable material they can serve as a temporary scaffold for externally produced implants seeded by cells. In such case, artificial nanofibrous scaffold is gradually digested by the cells and replaced by a native collagen matrix.

Implantable devices made of micro-nanofibers are supporting guided cells growth for the use in regenerative medicine to rebuild damaged, worn or aged tissue. For such types of applications, electrospun nanofibers have been tested for the urinary bladder wall regeneration, bone scaffold coatings, scaffolds for skin regeneration, post-surgery barrier material [e.g. 3]. Nanofibers are manufactured at a room temperature that enables to produce membranes made of temperature-sensitive materials (e.g. polyhydroxyesters or proteins) [19]. Different types of drugs or even living cells can be incorporated into the material. Materials of biological significance are produced by the electrospinning process [11,25].

The aim of our present study was to examine the influence of the wound dressing material made of electrospun nanofiber membrane (nanofiber mat/net) on injured brain parenchyma in an SBI rat model.

Material and methods

All applied routines involving animals were authorized by the 4th Local Animal Experimentation Ethics Committee and were compatible with European Union regulations governing the care and use of laboratory animals. Animals were kept in precisely specified and controlled conditions: in 60-70% relative humidity and temperature 20°C at 12 h/12 h light/dark cycle (lights on at 7 a.m.), and were fed on standard food for laboratory rodents (Ssniff M-Z, ssniff Spezialdiäten GmbH, Soest, Germany) and purified tap water *ad libitum*. Experiments were carried out on adult Wistar male rats, weighing at the beginning of the experiment 200-250 g. Animals were divided into five experimental groups:

1) control, intact animals (sacrificed in the following time points: 4, 7, 14 and 30 day of the experiment; 7 animals for each investigated time point),
2) animals with applied biodegradable nanofiber dressings on the surface of undamaged cerebral cortex (sacrificed in the following time points: 4, 7, 14 and 30 day of the experiment; 7 animals for each investigated time point),
3) animals with the surgical injury of the cerebral cortex made (sacrificed in the following time points: 4, 7, 14 and 30 day of the experiment; 7 animals for each investigated time point),
4) sham-operated animals (full procedure of the scull trepanation was conducted) sacrificed in the following time points: 4, 7, 14 and 30 day of the experiment; 7 animals for each investigated time point,
5) animals with the surgical injury made with applied biodegradable nanofiber dressings on the surface of postoperative wound (sacrificed in the following time points: 4, 7, 14 and 30 day of the experiment; 7 animals for each investigated time point).

Nanomaterials used in our study were produced by electrospinning of poly (L-lactide-*co*-caprolactone) (PLCL, containing 70% L-lactide and 30% caprolactone units) purchased from Purac Biochem BV, Gorinchem, the Netherlands, and dimethylformamide (DMF) purchased from POCH, Poland. All of the materials were used without any further purification. The electrospinning process was performed according to the procedure described in detail earlier [19]. Briefly, the electrospinning solution was made of 9% of PLCL dissolved in 1:9 (wt/wt) mixture of DMF and $CHCl_3$. The solution flow rate was fixed at 500 µl/h, positive electric potential of the 0.75 kV/cm was applied to the needle and spinning distance was 20 cm. The resulting polymer nanofibers were collected on a rotating drum (3000 rpm) covered with aluminium foil. The structure of the mat was examined by the Scanning Electron Microscopy (SEM, Jeol, JSM 6390 LV, Japan). Fibers were sputtered with a gold (mini sputter coater SC 7620, Polaron, United Kingdom) and the thickness of fibers and whole mats were analyzed. The thickness of fibers was 0.5-2.3 µm and the size of investigated mats was 80-120 µm. Porosity of the material was calculated by dividing the density of the nanofibrous mat (net) by PLCL density (1.17 g/cm^3), according to the method presented by Lee, it was 69% [22].

Neurosurgical damage of some part of the somatosensory cerebral cortex was performed according to the procedure described previously [7]. In short, the operation of surgical injury of the cerebral cortex was performed under deep anaesthesia (20 mg/kg ketamine hydrochloride). After the skin was incised, the frontal bone was trepanned 2 mm laterally from the bregma and 2 mm anteriorly to the coronal suture and the meninges was incised. The operated cortex (a 2 × 2 × 2 mm region of the somatosensory cortex) was hemisected with a small scalpel and the wound was closed. The skin wound was sutured. After the operation, the animals were placed in standard animal house conditions under the experimenter's care. After the above specified survival times the animals were perfused and material collected from their brains was evaluated using techniques of light and electron microscopy (see below).

All animals were deeply anesthetized using Nembutal (80 mg/kg b.w., i.p.) and perfused by the ascending aorta, initially applying 0.9% NaCl in 0.01 M sodium-potassium phosphate buffer pH 7.4 (PBS), and afterwards with 'regular' ice-cold fixative (with 4% formaldehyde in 0.1 M phosphate buffer pH 7.4 for light microscopy or with 2% paraformaldehyde and 2.5% glutaraldehyde in 0.1 M cacodylate buffer, pH 7.4 for transmission electron microscopy), as described earlier [7]. Following the perfusion, the brains were taken away from the sculls to be immersed for 2 h in the same fixing agent. Afterwards, the brains were saturated with sucrose through immersing in 10, 20 and 30% (w/v) sucrose solutions in PBS and cut to 40 µm-thick free-floating coronal sections applying a cryostat (CM 1850 UV, Leica, Germany). In the next step, the sections were prepared for immunohistochemical (IHC) studies.

Free-floating brain sections were preincubated with 3% normal goat serum solution in PBS supplemented with 0.2% Triton X-100 (PBS+T). Subsequently, the sections were incubated for 1 h at 37°C with PBS+T containing 1% normal goat serum and following primary antibodies (Abs): 1) murine monoclonal Ab against NeuN (Chemicon, USA, dil. 1 : 1000); 2) murine monoclonal Ab against GFAP (Chemicon, USA, dil. 1 : 1000); 3) murine monoclonal Ab against Vimentin (Santa Cruz, USA, dil. 1 : 400) and 4) murine monoclonal Ab against macrophages (Santa Cruz, USA, dil. 1 : 400). The reaction was terminated by washing the sections with PBS+T. Next, the sections were incubated for 1 h at 37°C with the respective secondary Abs. The secondary Abs used were as follows: 1) goat anti-mouse antibody

conjugated with Alexa Fluor 594 (Invitrogen, USA, dil. 1 : 100) or 2) goat anti-mouse antibody conjugated with HRP (Bio Rad, USA, cat. no. 170-5047, dil. 1 : 1000; and the reaction was visualized using DAB as a chromogen). Finally, the sections were rinsed with PBS+T, mounted on silanized glass slides (Sigma) and covered with Vectashield mounting medium for fluorescence microscopy (Vector Labs Inc., Burlingame, CA, USA).

Immunostaining was detected with a model Optiphot-2 Nikon fluorescent microscope (Japan) equipped with the appropriate filters, and recorded with a model DS-L1 Nikon camera (Japan). Specificity of the immunostaining was verified by performing a control ("blank") staining procedure with primary antibodies omitted in the incubation mixture. No staining was observed in these control sections.

Morphology of cell nuclei was examined on brain sections mounted on microscope slides. Sections were washed in PBS and incubated in a 1 µg/ml solution of Hoechst stain (bisbenzimide dye, No 33258, B-2883, Sigma; prepared in PBS) for 2 min at room temperature. The stain was then drained off and cover slipped with PBS for visualization.

Tissue specimens for electron microscopy analyses were collected from rats anesthetized and perfused as above. The tissue specimens for electron microscopy analyses were collected from the cerebral cortex bordering the surgical cortical injury in the operated rats and from the related cortex part in the control rats. The specimens were handled with the typical ice-cold fixative (see above) post-fixed in 1% (w/v) OsO_4 solution in deionized water, dehydrated in an ethanol gradient, and at last encased

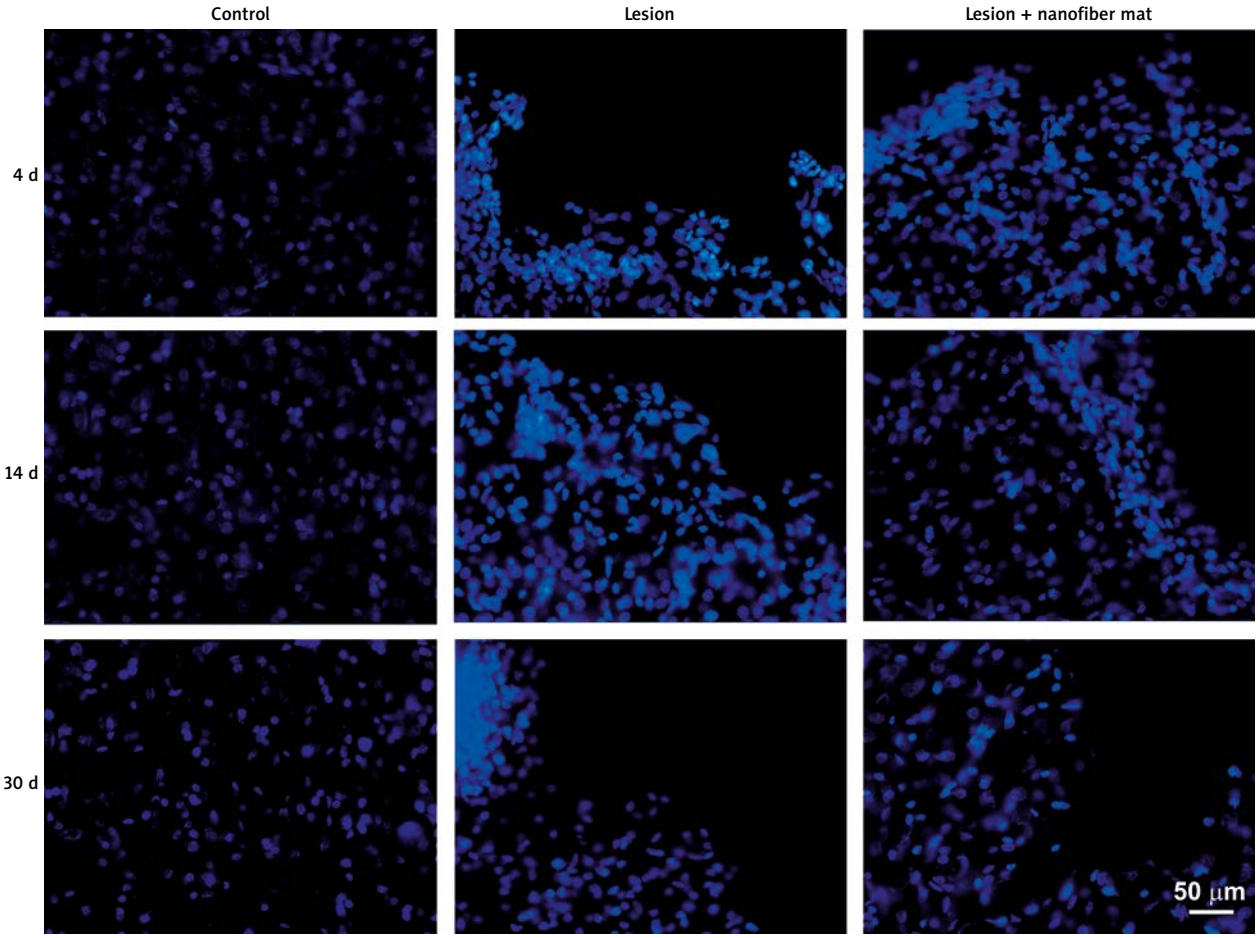

Fig. 1. Hoechst labelling of cell nuclei. The control cortex shows the presence of numerous nuclei with unchanged morphology (left panel). The lesioned cortex shows many cells with pyknotic nuclei revealed by intense fluorescence (middle panel). Application of the poly-caprolactone nanofiber mat at the time of the lesion (right panel) hampers the changes in the nuclear morphology.

in epoxy resin (Epon 812). Ultrathin (60 nm) sections were prepared as described earlier [8]. Material was examined in a transmission electron microscope (JEM-1200EX, Jeol, Japan).

GFAP-positive structures (processes and somata) forming the glial scar on the wound were examined using the Scion Image software (Scion Corp.). The GFAP-positive structures are reduced to a single pixel in width.

Results

Brain sections of intact control animals (experimental group 1) from all investigated time points revealed a proper morphological structure of all composing elements of the neurovascular unit: neurons, astrocytes and capillary blood vessels (Figs. 1-5). Similar results were obtained in the respective samples from sham-operated animals – experimental group 4 (data not shown).

Analysis of samples from the rats with nanofiber net dressing placed on the surface of intact neocortex (experimental group 2) has demonstrated no major changes in the examined structures (data not shown). In particular, there were neither neurodegeneration nor inflammatory reaction in the brain cortex as evidenced by the absence of macrophages. We also did not detect any activated astro- and microglial cells, only a slight increase in the number of GFAP-positive astrocytes was found in the vicinity of the dressing, but the cells showed no signs of hypertrophy (data not shown).

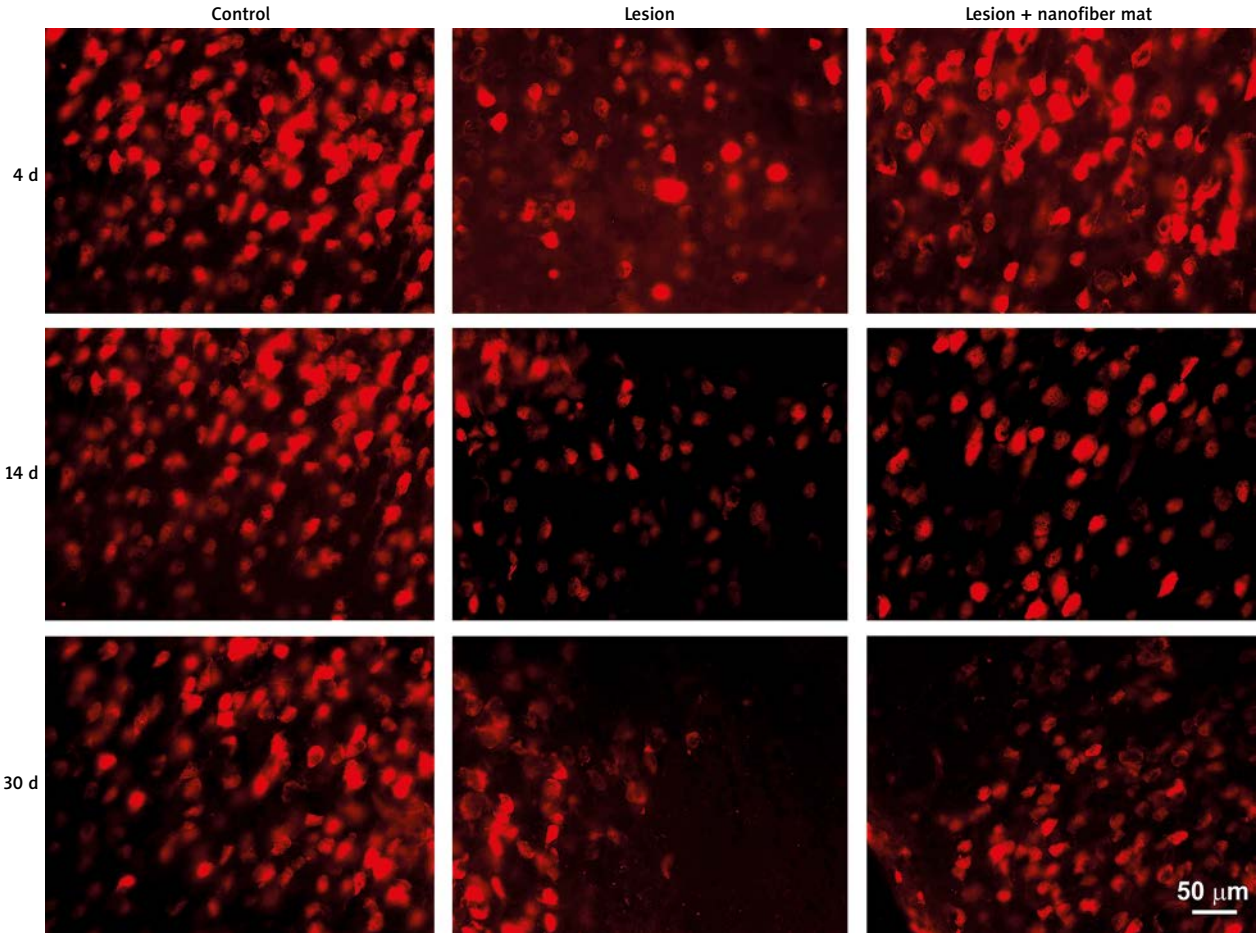

Fig. 2. NeuN immunostaining of rat cerebral cortex. Cortical sections derived from control animals (left panel) show the presence of numerous intensively stained neurons. Material from the damaged cortex (middle panel) shows a major decrease in staining intensity and in the number of labelling cells. Sections from brains dressed with nanofiber nets (right panel) show many neurons revealing intense immunosignal in all investigated time points.

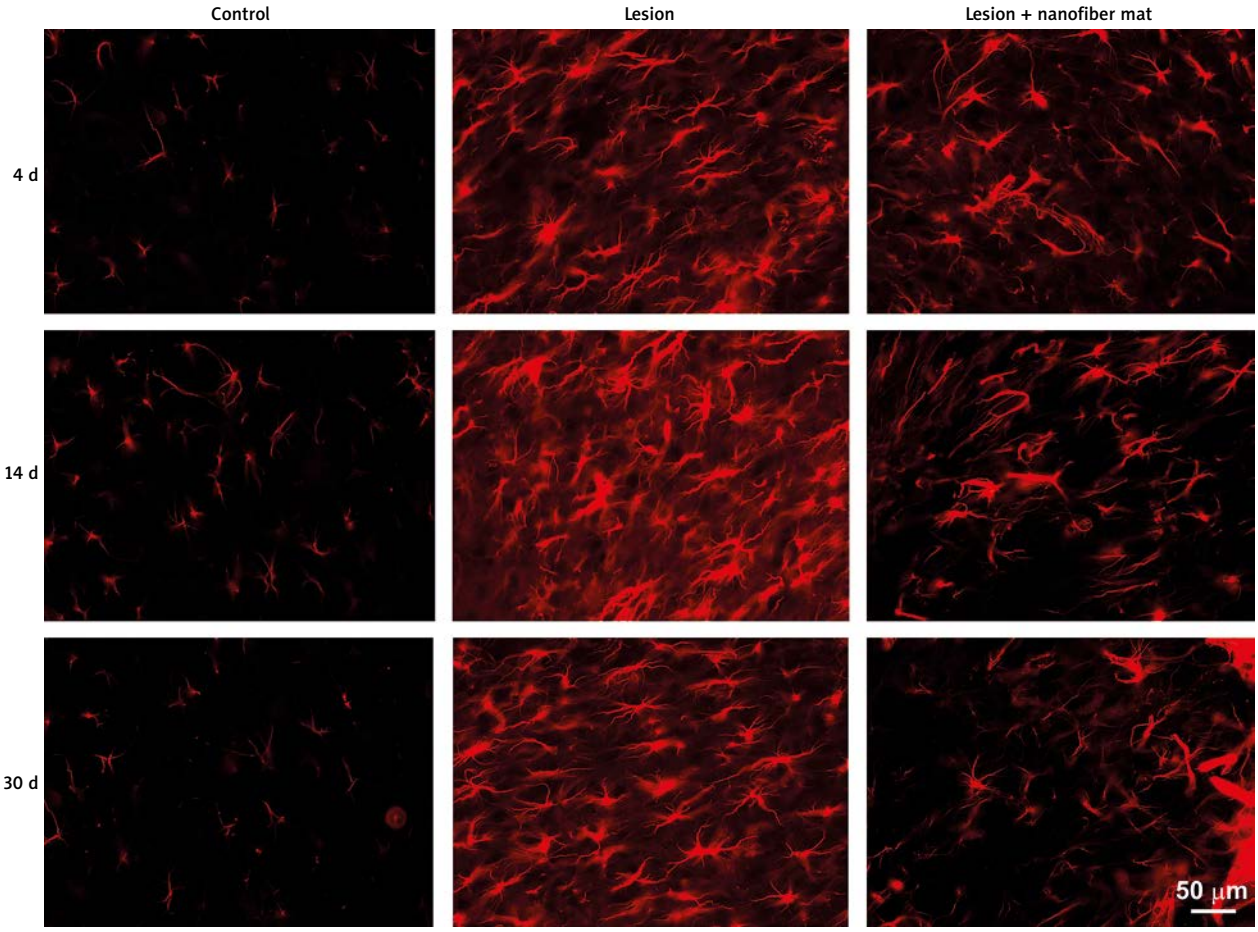

Fig. 3. GFAP immunostaining within the cerebral cortex area located distant to the lesion. Sections from the control cortex show scanty GFAP immunoreactivity (left panel). In the lesioned cortex, a massive increase in GFAP signal and astrocyte activation is visible (middle panel). Following the application of the nanofiber mat, the number of astrocytes and the intensity of GFAP signal were smaller than those observed in the injured animals (right panel).

Brain sections from rats subjected to the surgical lesion of the cerebral cortex (experimental group 3) showed massive death of neuronal cells (Figs. 1 and 2), which was most intense between 4 and 14 days post-surgery, and were associated with macrophage influx from the site of the trauma (Figs. 5C and 6). Electron microscopic data confirmed and extended that result. We found many macrophages localized in the vicinity of the lesion. We also detected numerous neurons dying *via* apoptosis and only few apoptotic astrocytes (data not shown).

Starting from the early post-surgery times (4 days post-lesion) a massive hypertrophy of astrocytes was seen in the perilesional cortical area (Fig. 7). The same phenomenon was observed in the area located at some distance to the injured tissue (Fig. 3). The scar-forming GFAP-immunoreactive (GFAP-IR) cells observed in the later post-operative time points were highly hypertrophied (Fig. 7), and some of the scar-forming astrocytes were vimentin-positive (Fig. 8). Some of the astrocytes located in the distance to the damaged cortical region were vimentin-positive too (Fig. 4). The activation of astroglial cells and glial scarring were associated with the formation of new capillary blood vessels in the perilesional area (Fig. 9). Thirty days post-lesion the scar formed at the site of the trauma showed signs of destabilization and secondary degeneration (Fig. 9B).

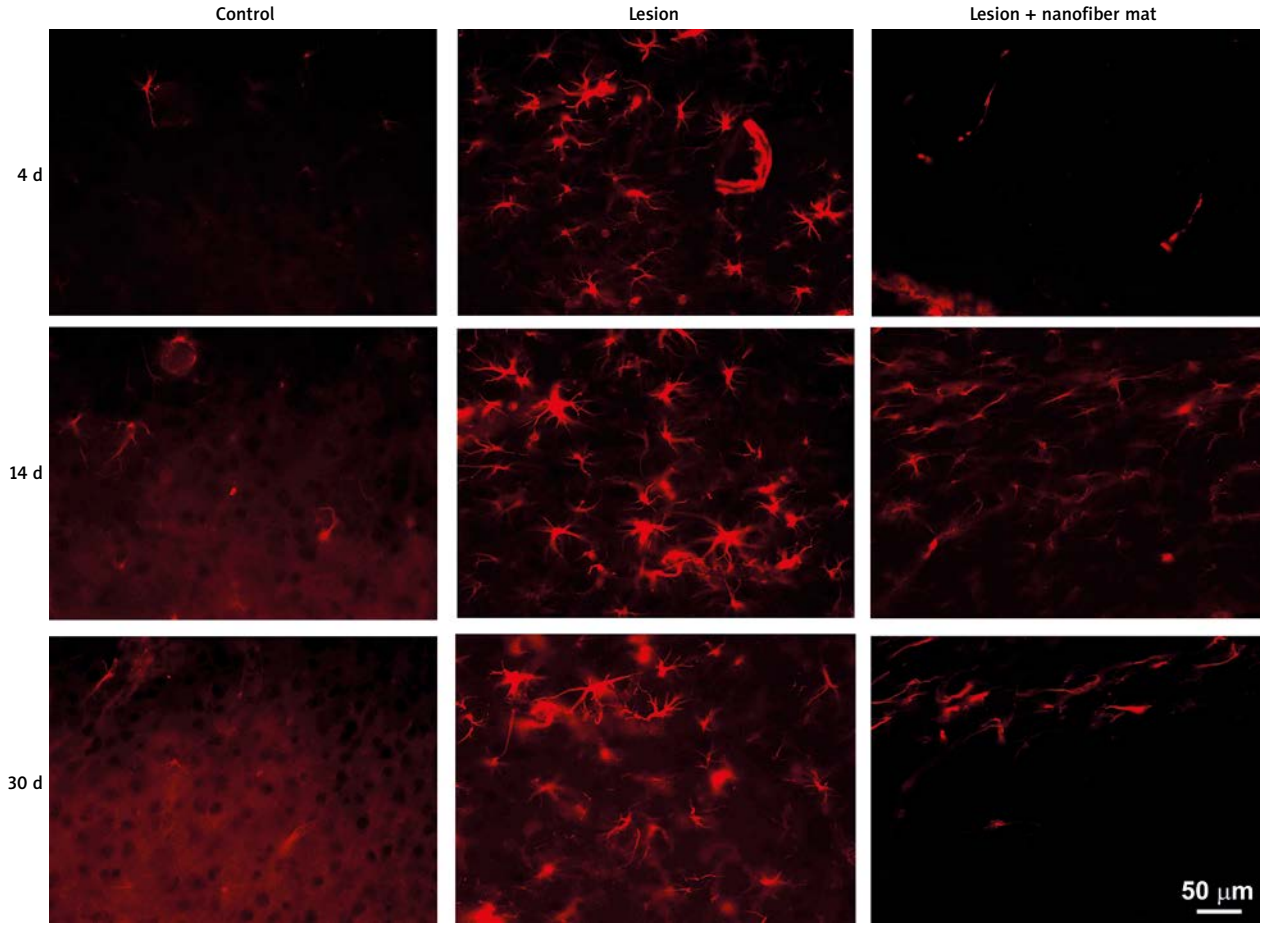

Fig. 4. Vimentin immunostaining within the cerebral cortex area located distant to the lesion. In the control cortex, negligible vimentin immunoreactivity was observed (left panel). The injured cortex revealed increase in the staining intensity (middle panel). Application of the nanofiber mat (right panel) counteracts the change.

The analysis of brain sections from the rats subject to surgical neocortex lesion that has been dressed with the nanofiber net (experimental group 5) showed only weak inflammatory signs. In particular, no macrophage infiltration or only single macrophages were found in the investigated brain area (Figs. 5D and 6).

There was also no formation of new blood vessels and no massive glial scarring (Fig. 5D). Several induction of astroglia (GFAP- or vimentin-positive cells) (Figs. 3, 4 and 7, 8) and formation of a subtle, barely visible glial scar on the surface of the lesioned neocortex were observed. Additionally, the glial scar was much thinner than that observed in the lesioned brains without dressing with nanofiber mat. Its structure was also much more "orderly" (see Figs. 5D, 7 and 8).

The GFAP immunoreactive structures (perikarya and cell processes) were analyzed with use of the Scion Image software, where these structures were reduced to a single pixel in thickness (Fig. 10).

Discussion

Membranes manufactured using the electrospinning method have bounded permeability, particularly for cells, however, permanent drainage of their decomposition products is kept. Besides, nutrient, oxygen and metabolites diffuse with ease through the membrane. The above membranes were made of micro- and nanofibers, which – because of their similarity to the Extracellular Collage Matrix – are treated as a natural environment by cells. The electrospun membranes are composed of polyester which gained medical approval: poly(L-lactide-*co*-caprolac-

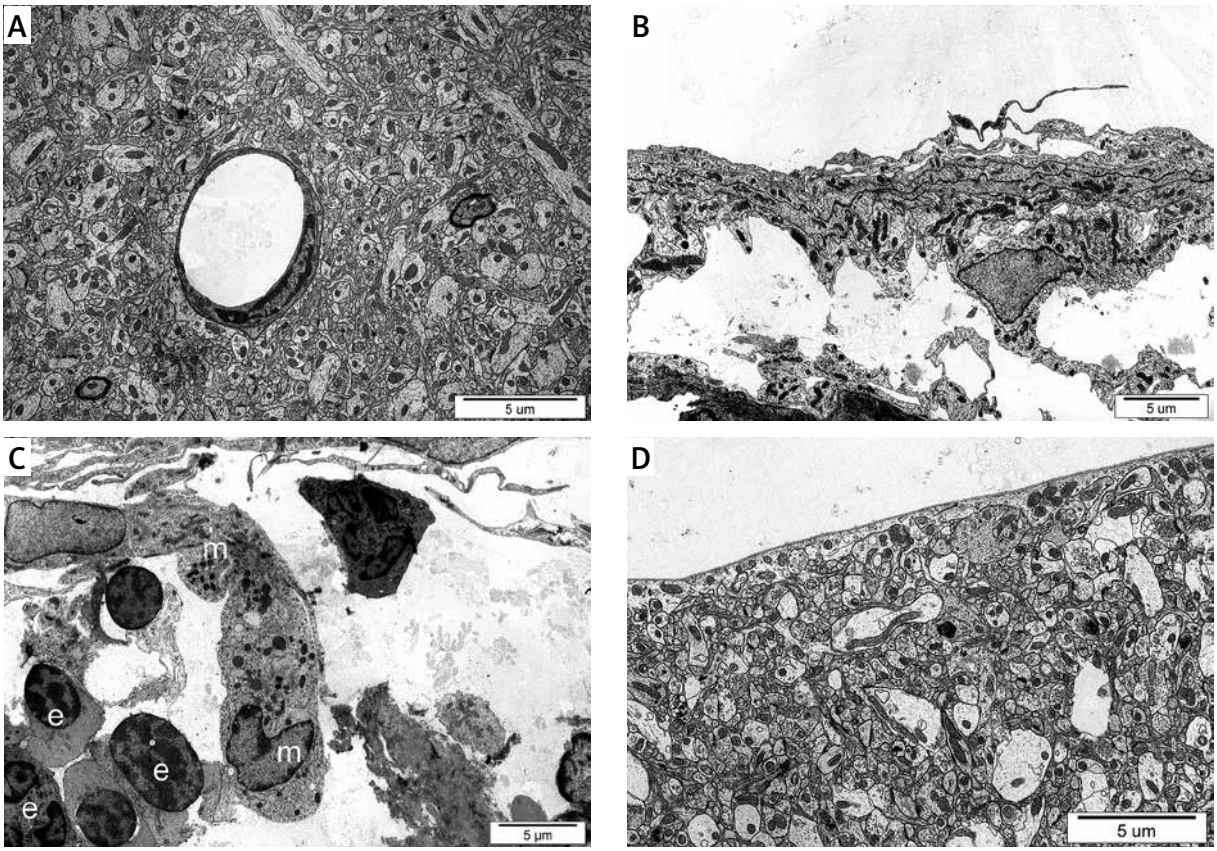

Fig. 5. Electronograms of the control (sham-operated, **A)** and lesioned cerebral cortex **(B-D)**; 4 days post-lesion. Electronogram B reveals massive glial scarring observed in the absence of the nanofiber net in the cortical molecular layer. The zone above the lesion **(C)** shows the presence of macrophages (m) and probably lymphocytes (e). Nanofiber net application at the time of the lesion attenuates the scarring and prevents infiltration of morphotic blood elements **(D)**. Electronogram D shows a part of the cortical molecular layer.

tone) (PLCL). PLCL is a copolymer of lactic acid and 6-hydroxyhexanoic acid. The electrospun mat was used to protect damage brain tissue from further progressing injury in the SBI rat model. Gradual biodegradation (12-24 months) of the mat was supposed to promote the correct healing process.

There are two kinds of products of membrane degradation: natural metabolite (lactic acid) and its analogue (6-hydroxyhexanoic acid). By reason of chemical character, both of acids in high concentrations have an irritating action to tissue. Lactic acid (pKa = 3.83) is eight times stronger than its non-toxic analogue – 6-hydroxyhexanoic acid (pKa = 4.75). Although the fibrous mat maintained strength comparing to the solvent-cast membrane, it was created from far less material. Thanks to contact of the damaged tissue with far less irritating hydroxy acids (produced during hydrolysis), inflammation is presumed to be much lower. Solvent-cast polymeric membranes accumulate hydroxy acids which were formed during the *in vivo* hydrolytic degradation of polyhydroxy acid (PHA), monomeric hydroxy acids. These acids play an autocatalytic role, that is they accelerate the process of hydrolytic degradation what in consequence causes faster degradation of thicker materials. The fibrous structure is also a key issue for the stability of the membrane. The nanofibrous mat is easily emptied by biological fluids and do not accumulate hydroxy acids. A class of biopolymers, aliphatic polycarbonates, which was widely studied by the authors before [26-29], creates a very weak carbonic acid during the hydrolytic degradation and therefore is free from the problem of autocatalytic hydrolysis.

Nanomaterials have a huge potential for the new techniques in the tissue engineering. The aim of tis-

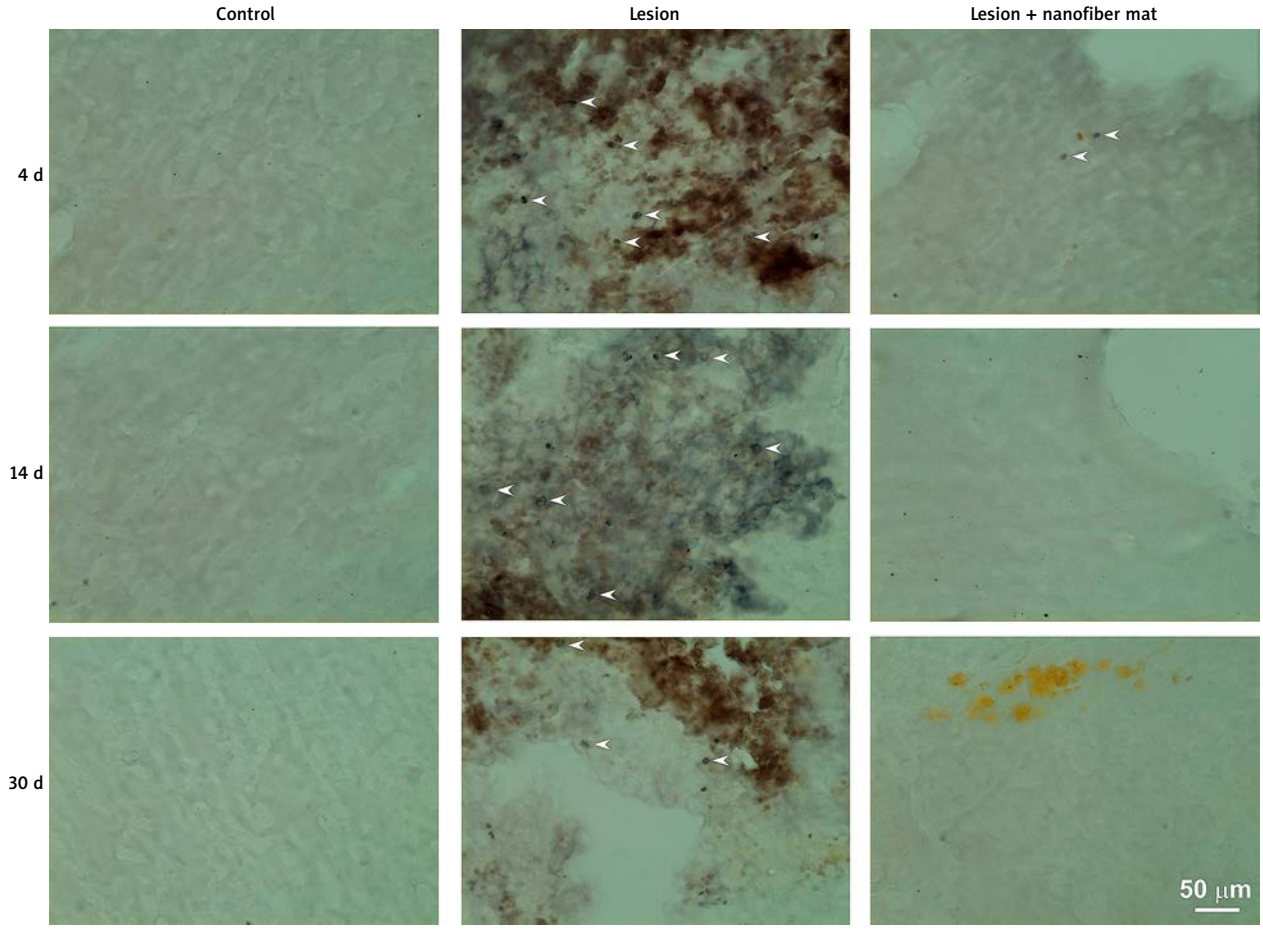

Fig. 6. Macrophages immunostaining. Macrophages in the cerebral cortex. In the control cortex we did not find any macrophages (left panel), but numerous macrophages were detected in the lesioned cortex (middle panel). Tissue dressed with the nanofiber mat (right panel) show only few macrophages at the early experimental time point.

sue engineering and regenerative medicine is to produce a biological substitute in order to restore, maintain or repair damaged tissue and organ functionality.

Our preliminary research employs the electrospun nanofiber mat in order to prevent nervous tissue from cicatrization after surgical injury. Glial scar formed after brain injury is an effective barrier preventing regeneration of the damaged area of the brain. Moreover, delayed consequences of such injuries are reported [31]. Prevention of nervous tissue from cicatrization leads to its better post-damage condition.

Our model imitates well the respective human neurosurgery situation and involves the most typical consequences of SBI, such as brain oedema and neuronal death. The model makes it possible to study various processes accompanying the course of repairing and rebuilding the damaged area of the brain at different time intervals after the injury.

The results obtained from intact animals (experimental group 1) analyzed at all experimental time points show proper morphology of all neurovascular unit components. Similar data were obtained from the brains derived from animals of experimental group 2 (animals with the nanofibrous mat applied on the undamaged cerebral cortex). These data let us to suppose that the nanofiber nets did not evoke inflammation, e.g. they meet the first criterion to be used as a material for medical applications.

Results of analysis of material harvested from animals of experimental group 4 (sham-operated rats) were similar to results of the control group.

Results of experimental group 3 (animals with performed surgery) revealed that surgical injury

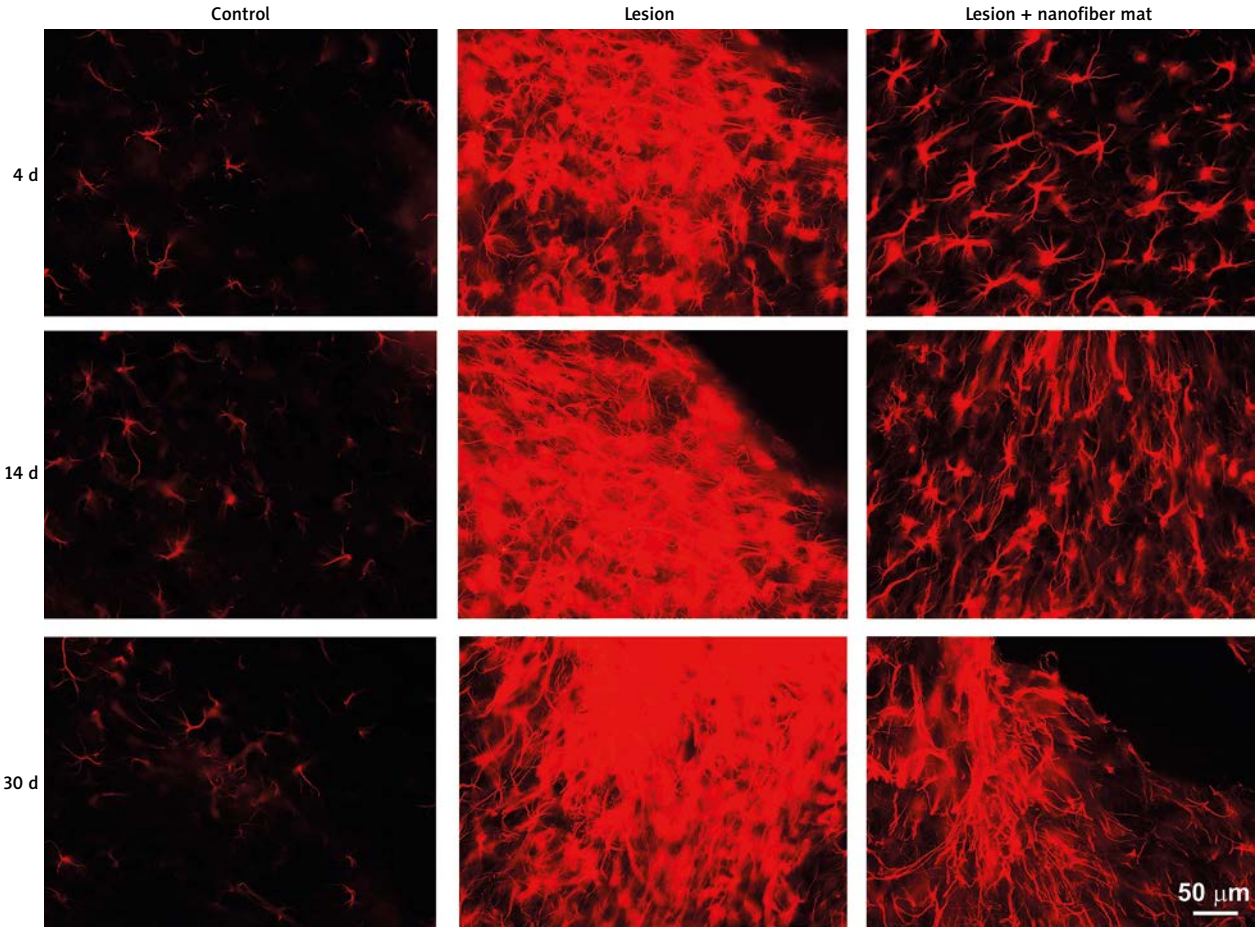

Fig. 7. GFAP immunostaining of the cortical region adjacent to the lesion. The control cortex shows scanty GFAP immunoreactivity (left panel). The cortical lesion induces massive increases in the staining and astrocyte activation (middle panel). Application of the nanofiber mat (right panel) counteracts the changes.

of the cerebral cortex leads to degeneration and death of cells close to the wound. Afterwards, it also affects areas distant to the lesion [32]. In the cortex of animals of this group we detected numerous dying neurons with features indicating apoptosis (highly condensed nuclear chromatin, the presence of apoptotic cells) as well as necrosis (cells bloating, defecting of cell organelles). Our data confirmed the results of other investigators [6].

The trauma also disrupted the blood-brain barrier (BBB), which enabled massive migration of blood cells and serum into the wound area. Disruption of the BBB was an early feature of lesion formation leading to oedema, excitotoxicity and entry of serum proteins and inflammatory cells [11]. It is known that damage to the endothelium of blood vessels is a known pathway for initiation of inflammation. Monocytes from the bloodstream enter peripheral tissue and transform into macrophages, which are the primary phagocytes of the immune system [12].

At four days after the surgery we registered a considerable number of macrophages on the analyzed area of the cerebral cortex.

Astrocytes take part in all forms of CNS insults (e.g. trauma or ischemia) by a process commonly referred to as reactive astrogliosis. This process results in scar formation [30]. Reactive astrogliosis plays an essential role in orchestrating the (brain) injury response as well as in regulating inflammation and repair. In the analyzed model of brain damage as early as 4 days after injury, a massive astrogliosis appears and at later post-lesion time points, glial scar formation starts at the place of damage [7].

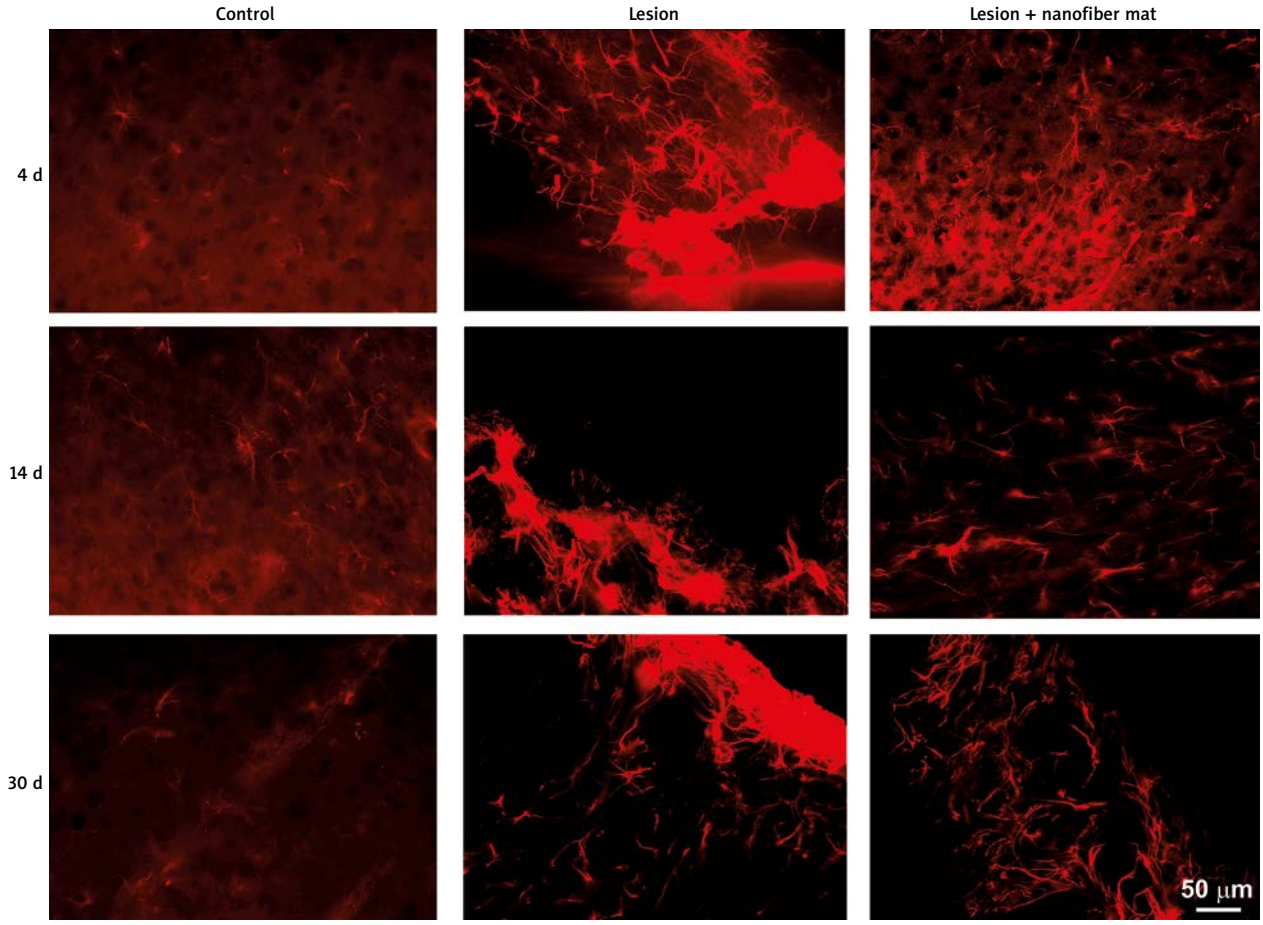

Fig. 8. Vimentin immunostaining of the cortical region adjacent to the lesion. The left panel shows sections from the control cortex with only weak vimentin immunoreactivity, opposite to the heavy immunoreaction visible in the injured cortical area (middle panel). Application of the nanofiber membrane (right panel) counteracts the changes.

Electron-microscopic (TEM) observations confirmed the light microscopic findings.

Numerous active astrocytes were part of the glial scar (GFAP- positive and Vim-positive) and possessed distinct attributes of hypertrophy. Astrocytes were arranged randomly and form a thick multilayer structure on the surface of the damaged cerebral cortex. Recent studies indicate the ambiguous role of reactive astrocytes in the formation of glial scars after the injury. On the one hand, it forms an effective barrier precluding the regeneration of nerve fibers on the damaged area, but on the other hand, it also precludes penetration of blood elements, which could additionally deepen the processes of degeneration through intensification of inflammatory processes in the tissue [16]. The contribution of immature (Vim-positive) astrocytes, occurring in the scar, in the promotion of regeneration after damage is also postulated. Nevertheless, our experiments conducted for an extended time after injury demonstrated that the glial scar is not a stable structure at this scale of time. Just 30 days after the operation, the initiation of scar decomposition and delayed degeneration in the area adjacent to the scar was observed. Considering these results we believe that the inhibition of reactive astrogliosis may be a useful therapeutic target in some situations.

At early postoperative time (4 days), the formation of new blood vessels in the area adjacent to the damage was observed. Nascent blood vessels, however, were morphologically anomalous to a high degree, which indicates its dysfunctionality. Most of them showed no pericytes in the vessel wall.

The main target of current research was to examine if the electrospun nanofiber mat may be useful as

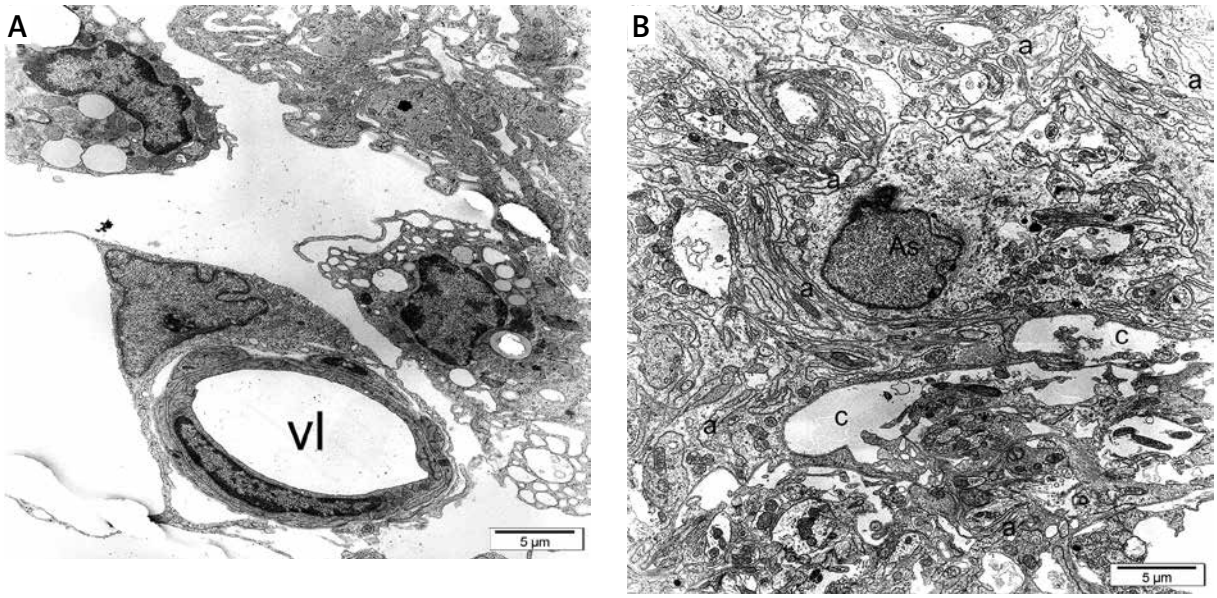

Fig. 9. Electronograms of the lesioned cerebral cortex. Electronogram **A** shows a new blood vessel formed in the peri-lesion zone, 14 days post-lesion; "vl" denotes vessel lumen. Electronogram **B** shows the glial scar region, 30 days post-lesion. Note signs of scar destabilization: astrocyte (As) and astrocytic processes (a) with signs of swelling, "c"s denote cavities formed due to glial scar decay.

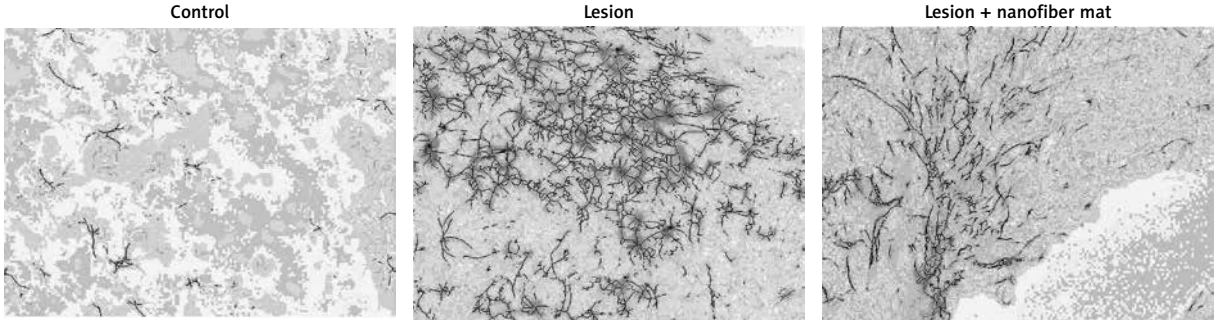

Fig. 10. Skeletonization of GFAP immunoreactive processes and somata. Note the highest density of GFAP-positive structures in the lesioned cortex with no nanofiber net application.

a barrier material preventing from cicatrization of the brain parenchyma. A massive astrogliosis observed in the experimental group 3 was not detected in the brains derived from animals with the nanofiber mat applied on the injured cortex (experimental group 5). Observed astrocytes did not show any signs of hypertrophy. Interestingly, a glial scar was formed by astrocytes organized in a more "orderly" manner than that observed in experimental group 3. The scar was also much thinner and had an ordered character. No influx of macrophages was observed in the area of damaged tissue. It suggests that the nanofiber net may protect tissue against the cascade of uncontrolled damage resulting from excessive proliferation of astrocytes and inflammation initiated. We suppose that the structure of the nanofiber mat can also simulate the structure of extracellular collagen matrix for the damaged tissue and have an influence on the lesion to particular components of the neurovascular unit. This would mean that the material simulating regular environment of extracellular matrix may modify the response of cells to the surgical injury. Furthermore, the main product of the nanofiber mat degradation, lactic acid, is postulated as a neuroprotective factor [2].

Conclusions

The nanofiber net used in this study is biocompatible and favourably modifies local inflammation

and cicatrization. Our results suggest that such nanofibers could be useful in neurosurgery.

Acknowledgements

This study was supported by the National Centre for Research and Development Project #NR13-0081-10-2010.

References

1. Barnes CP, Sell SA, Boland ED, Simpson DG, Bowlin GL. Nanofiber technology: designing the next generation of tissue engineering scaffolds. Adv Drug Delivery Rev 2007; 59: 1413-1433.
2. Berthet C, Lei H, Thevenet J, Gruetter R, Magistretti PJ, Hirt L. Neuroprotective role of lactate after cerebral ischemia. J Cereb Blood Flow Metab 2009; 29: 1780-1789.
3. Bretcanu O, Misra SK, Yunos DM, Boccaccini AR, Roy I, Kowalczyk T, Błoński S, Kowalewski TA. Electrospun nanofibrous biodegradable polyester coatings on Bioglass®-based glass-ceramics for tissue engineering. Mater Chem Phys 2009; 118: 420-426.
4. Bruns JR, Hauser WA. The epidemiology of traumatic brain injury: a review. Epilepsia 2003; 44 (Suppl 10): 2-10.
5. Cole TB. Global road safety crisis remedy sought: 1.2 milion killed, 50 milion injured annually. JAMA 2004; 291: 2531-2532.
6. Cruchten S, van den Broeck W. Morphological and biochemical aspects of apoptosis, oncosis and necrosis. Anat Histol Embryol 2002; 31: 214-223.
7. Frontczak-Baniewicz M, Chrapusta SJ, Sulejczak D. Long-term consequences of surgical brain injury – characteristics of the neurovascular unit and formation and demise of the glial scar in a rat model. Folia Neuropathol 2011; 49: 204-218.
8. Frontczak-Baniewicz M, Walski M. New vessel formation after surgical brain injury in the rat's cerebral cortex. I. Formation of the blood vessels proximally to the surgical injury. Acta Neurobiol Exp 2003; 63: 65-75.
9. Frontczak-Baniewicz M, Walski M. Glial scar instability after brain injury. J Physiol Pharmacol 2006; 57 (Suppl 4): 97-102.
10. Frontczak-Baniewicz M, Sulejczak D, Andrychowski J, Gewartowska M, Laure-Kamionowska M, Kozłowski W. Morphological evidence of the beneficial role of immune system cells in a rat model of surgical brain injury. Folia Neuropathol 2013; 5: 324-332.
11. Fryczkowski R, Kowalczyk T. Nanofibres from polyaniline/polyhydroxybutyrate blends. Synth Met 2009; 159: 2266-2268.
12. Geissmann F, Manz MG, Jung S, Sieweke MH, Merad M, Ley K. Development of monocytes, macrophages, and dendritic cells. Science 2010; 327: 656-661.
13. Giunta B, Obregon D, Velisetty R, Sanberg PR, Borlongan CV, Tan J. The immunology of traumatic brain injury: a prime target for Alzheimer's disease prevention. J Neuroinflammation 2012; 9: 185.
14. Hillier SL, Hiller JE, Metzer J. Epidemiology of traumatic brain injury in South Australia. Brain Inj 1997; 11: 649-659.
15. Jablonska A, Lukomska B. Stroke induced brain changes: implications for stem cell transplantation. Acta Neurobiol Exp 2011; 71: 74-85.
16. Kamel H, Iadecola C. Brain-immune interactions and ischemic stroke: clinical implications. Arch Neurol 2012; 69: 576-581.
17. Kiraly MA, Kiraly SJ. Traumatic brain injury and delayed sequelae: a review-traumatic brain injury and mild traumatic brain injury (concussion) are precursors to later-onset brain disorders, including early-onset dementia. Scientific World Journal 2007; 7: 1768-1776.
18. Koskinen S, Alaranta H. Traumatic brain injury on Finland 1991-2005; a nationwide registered study of hospitalized and fatal TBI. Brain Inj 2008; 22: 205-214.
19. Kowalczyk T, Nowicka A, Elbaum D, Kowalewski TA. Electrospinning of bovine serum albumin. Optimization and the use for production of biosensors. Biomacromolecules 2008; 9: 2087-2090.
20. Kowalewski TA, Barral S, Kowalczyk T. Modeling electrospinning of nanofibers. In: Pyrz R, Rauhe JC (eds.). IUTAM Symposium on modeling nanomaterials and nanosystems. Springer 2009; 13: 279-292.
21. Langlois JA, Sattin RW. Traumatic brain injury in the United States: research and programs of the Centers for Disease Control and Prevention (CDC). J Head Trauma Rehabil 2005; 20: 187-188.
22. Lee JB, Jeong SI, Bae MS, Yang DH, Heo DN, Kim CH, Alsberg E, Kwon IK. Highly porous electrospun nanofibers enhanced by ultrasonication for improved cellular infiltration. Tissue Eng Part A 2011; 17: 2695-2702.
23. Li H, McDonald W, Parada I, Faria L, Graber K, Takahashi DK, Ma Y, Prince D. Targets for preventing epilepsy following cortical injury. Neurosci Lett 2011; 497: 172-176.
24. McKee AC, Cantu RC, Nowinski CJ, Hedley-Whyte ET, Gavett BE, Budson AE, Santini VE, Lee HS, Kubilus CA, Stern RA. Chronic traumatic encephalopathy in athletes: progressive tauopathy after repetitive head injury. J Neuropathol Exp Neurol 2009; 68: 709-735.
25. Reneker DH, Yarin AL, Zussman E, Xu H. Electrospinning of nanofibers from polymer solutions and melts. In: Aref H, VanDerGiessen E (eds.). Advances in Applied Mechanics 2007; 41: 43-195.
26. Rokicki G, Kowalczyk T. Cyclic carbonates and spiro-orthocarbonates - perspective monomers in the polymer chemistry of polymers. Polimery 1998; 43: 407-415.
27. Rokicki G, Kowalczyk T. Synthesis of oligocarbonate diols and their characterization by MALDI-TOF spectrometry. Polymer 2000; 41: 9013-9031.
28. Rokicki G, Kowalczyk T, Glinski M. Synthesis of six-membered cyclic carbonate monomers by disproportionation of 1,3-bis (alkoxycarbonyloxy) propanes and their polymerization. Polym J 2000; 32: 381-390.
29. Rokicki G, Piotrowska A, Kowalczyk T. Cyclic carbonates used in the synthesis of oligocarbonate diols involving step growth polymerization. Polimery 2001; 46: 483-493.
30. Rolls A, Shechter R, Schwartz M. The bright side of the glialscar in CNS repair. Nat Rev Neurosci 2009; 10: 235-241.
31. Shively S, Scher AI, Perl DP, Diaz-Arrastia R. Dementia resulting from traumatic brain injury. What is the patology? Arch Neurol 2012; 9: 1-7.

32. Sulejczak D, Grieb P, Walski M, Frontczak-Baniewicz M. Apoptotic death of cortical neurons following the surgical brain injury. Folia Neuropathol 2008; 46: 213-219.
33. Tomkins O, Feintuch A, Benifla M, Cohen A, Friedman A, Shelef I. Blood-brain barrier breakdown following traumatic brain injury: a possible role in posttraumatic epilepsy. Cardiovasc Psychiatry Neurol 2011; 2011: 765923; doi: 10.1155/2011/765923.
34. Willmore LJ. Posttraumatic epilepsy: What's contusion got to do with it? Epilepsy Curr 2012; 12: 87-91.
35. Ziemka-Nalecz M, Zalewska T. Endogenous neurogenesis induced by ischemic brain injury or neurodegenerative diseases in adults. Acta Neurobiol Exp (Wars) 2012; 72: 309-324.